Numerical and experimental investigation of a correlation model to describe spatial variability of concrete properties

Wouter Botte[a]*, Eline Vereecken[a] and Robby Caspeele[a]

[a] *Department of Structural Engineering and Building Materials, Ghent University, Belgium*

*Corresponding author: Wouter.Botte@UGent.be

Abstract – The heterogeneous character of concrete results in spatial variation of its material properties. Random field models are often used to account for this effect. Due to the large scatter on the correlation lengths suggested in literature, tests could be performed to determine the most appropriate correlation model and corresponding correlation length. Subsequently, different techniques can be employed to fit an analytical model to the experimental semivariogram resulting in the most appropriate correlation model and corresponding correlation length. However, the resulting correlation lengths can largely depend on the experimental design. In this work, the effect of several parameters and choices to be made by an engineer in deriving the correlation model based on experimental data from destructive tests has been investigated. It was found that the curve fitting method generally leads to better estimates of the scale of fluctuation compared to the maximum likelihood method. Moreover, there is a clear benefit of applying a bootstrapping procedure to the experimental data to estimate the covariance matrix adopted in the fitting procedures as well as to estimate the uncertainty related to the estimated parameters. When a measurement error is suspected to be present and cannot be neglected, the nugget should be estimated together with the variance and the scale of fluctuation. Furthermore, the Gaussian correlation model was found to be the most robust choice, even if the actual correlation model is not Gaussian. the latter was confirmed for actual experimental data on the material properties of concrete, where a linear model was found to fit the data best but the Gaussian model provided comparable results.

Introduction

Material properties of concrete are having some spatial variation due to the heterogeneous character of the concrete. To account for this spatial variation, random field models are often used. Nevertheless, there is no general consensus on which correlation model should be applied and what are the appropriate correlation lengths for different concrete properties. Variables often modelled by random fields are the concrete cover, surface chloride concentration, concrete compressive strength, critical chloride concentration, diffusion coefficient of the concrete, water/cement ratio, Young's modulus of the concrete, Poisson coefficient of the concrete, tensile strength of concrete, etc. (Vu & Stewart, 2005; Straub, 2011; Tran et al., 2012; Criel et al., 2014; Chen et al., 2018; Liang et al., 2022; Feng et al., 2022). There can be a large spread on the correlation lengths used for one variable, for example with ranges from 1 m to 3.5 m for the concrete cover and surface chloride concentration (Engelund, 1997; Vu, 2003; Li et al., 2004; Duprat, 2007; Stewart & Mullard, 2007). For the diffusion coefficient of concrete, suggested values for the correlation length range from 0.8 m to 2 m (Straub et al., 2009; Straub, 2011). Hence, it is not clear which correlation lengths should be used to model the spatial variation of the material properties of concrete.

Due to the large scatter on the correlation lengths suggested in literature, tests could be performed to determine the most appropriate correlation model and corresponding correlation length. Recently, some authors have proposed methods to recover the properties of the correlation structure using spatially sparse data based on advanced signal processing methods. Some successful applications of these methods can be found in e.g. Zhao & Wang (2020), He et al. (2021) and He et al. (2022). The current work focusses on a different approach frequently adopted in geosciences, in which an experimental semivariograms is derived from the experiments, providing an estimation of the correlation between measurements at specified distances from each other (i.e. lag distances). Subsequently, an analytical model is fit to such an experimental semivariogram, for which different techniques can be employed. Based on the results of this fitting procedure, the most appropriate correlation model and corresponding correlation length can be derived. However, the resulting correlation lengths can largely depend on the experimental design. For example, in (Zheng & Silliman, 2000) it is stated that a common 'rule' applied for the estimation of the correlation model is that at least 30 pairs of measurements are required for each lag distance in order to ensure a reliable semivariogram estimate (Matheron, 1965; Journel & Huijbregts, 1978). When using a uniform, square sampling grid, at least 200-300 measurements are needed in order to estimate the semivariogram reliably (Webster & Oliver, 1992). These rules of thumb lead to a very large number of measurements to be performed. This might be achievable in the application domains of the mentioned references (i.e. geosciences), but such a large number of measurements is not practical and unfeasible when considering measurements from destructive tests on concrete structures. Moreover, the requirements found for soil properties might differ from those for concrete, due to the differences in spatial variation (Cami et al., 2020; Yu et al., 2020; Tomizawa & Yoshida, 2022). Hence, in this work, it is investigated for what ratio of the correlation length to the structural length and for what sampling distances an appropriate estimate of the actual correlation model can be found. Such analyses have previously been executed in the field of geosciences. In (Christodoulou et al., 2021), the influence of the sampling domain length and the sampling interval on the correlation length has been investigated. Here it was found that the domain length strongly affects the results from the estimation of the correlation length, where larger domains improve the estimate. They also found that smaller intervals between the measurements improve the estimate of the correlation length. Hence, the current work investigates whether these results can be extended when applied to concrete structures.

In the abovementioned references, one single analytical correlation model has been assumed for the analyses. Nevertheless, it is often not known beforehand which correlation model is the most appropriate, and different correlation models can be fit to the experimental data, such as exponential and Gaussian correlation models. Each model might be assumed when fitting the correlation length to the experimental results, and the model with the best fit can be chosen as the most appropriate one. However, it might be that one model in general performs better than another correlation model. To the authors' best knowledge, such analyses have previously not been executed in existing literature.

Therefore, this will be investigated in the current work, considering the Gaussian and exponential correlation model since these are appearing most frequently in literature. In addition, the linear correlation model is considered because of its simplicity.

To fit an analytical correlation model to experimental data, different methods exist, such as the curve fitting method (Vanmarcke, 1977; Vanmarcke, 2010; O'Connor & Kenshel, 2013) and the maximum likelihood method (Li et al., 2004; O'Connor & Kenshel, 2013). In these methods, there can also be accounted for the uncertainty on the experimental data. One method to account for this uncertainty is by application of bootstrapping (Olea & Pardo-Igúzquiza, 2011). In this work, these different methods will be compared and it will be investigated whether one outperforms the others.

The outline of the paper is as follows: first, the experimental derivation of correlation models is explained, where first a short review on the topic of random fields is given, followed by an overview of different methods for fitting the correlation length to experimental data. Next, numerical analyses are performed to derive general guidelines for the most appropriate sampling pattern as a function of the structure length and the expected correlation length. Also, the different methods for the derivation of the correlation length are compared, together with different assumptions on the analytical correlation model. Moreover, different situations are considered, with varying assumptions on the standard deviation of the parameter of interest and on the measurement error. Finally, the processing of actual experimental data is treated and the correlation lengths are derived based on the different methods and recommendations derived from the theoretical analyses.

Experimental derivation of the correlation model

Parameters that are measured at different spatial coordinates are possibly correlated. To model this spatial correlation, random fields are often used. A brief introduction to random field modelling and the derivation of the appropriate correlation models based on experimental data is given in the sections below.

Definition of random fields

A random field $\{X(\mathrm{s}), \mathrm{s} \in \Omega\}$ is a function whose values are random variables for any position s in the domain $\Omega \subset \mathbb{R}^d$ (Vanmarcke, 2010). These random variables may have different characteristics for any point s in the random domain. A deterministic function $x(\mathrm{s})$ implies a single realisation of the random field $X(\mathrm{s})$. Two important features of a random field are the mean value μ_X or trend surface $m(\mathrm{s})$, and the covariance function $B(\mathrm{s}_i, \mathrm{s}_j)$ as given by equation (1). Here, σ^2 is the variance of the parameter under consideration.

$$B(s_i, s_j) = B\left(\left\|s_i - s_j\right\|\right) = B(\tau)$$
$$B(0) = \sigma^2 \tag{1}$$

This formulation, which only depends on the distance τ between two location vectors s_i and s_j, is valid when assuming homogenous, isotropic and ergodic fields. A summary of the covariance functions considered in this work is given in Table 1. The parameters θ and ρ_l designate, respectively, the scale of fluctuation and the correlation length. These parameters indicate the degree of spatial dependence in the random field. A large value for θ and ρ_l corresponds to a slowly varying field, while a small value represents a field characterised by a rapid spatial variation. The parameter c_0 represents the nugget, i.e. the value of the semivariogram at a lag distance τ equal to 0. This nugget effect quantifies the variability at distances smaller than the spacing of the measurements, including the measurement error. The latter effect is often neglected in scientific literature dealing with the assessment of spatial variability in concrete structures.

It should be pointed out that, when dealing with Gaussian random fields (i.e. the marginal distribution is a Gaussian or normal distribution), the mean μ_X and covariance function $B(\mathrm{s}_i, \mathrm{s}_j)$ are sufficient to completely specify the field.

In spatial data analysis of random fields, the use of a semivariogram $\gamma(s_j - s_i)$ is often preferred over the covariance function. A semivariogram contains the same information as the covariance function and the relation is described in equation (2), where $VAR[\cdot]$ and $COV[\cdot]$ are the variance and covariance operator, respectively.

$$2\gamma(s_j - s_i) = VAR[X(s_i) - X(s_j)] \\ = VAR[X(s_i)] + VAR[X(s_j)] - 2COV[X(s_i), X(s_j)] \tag{2}$$

This expression can be reduced for homogenous, isotropic and ergodic fields which are second-order stationary. The simplification is given by equation (3) and shows the relationship between the semivariogram and the covariance function.

$$\gamma(\tau) = c_0 + \sigma^2 - B(\tau) \tag{3}$$

Methods for determination of the correlation model

Different methods exist to determine the correlation model and correlation length based on an experimental dataset. In the following, two methods are described, i.e. the curve fitting (CF) method and the maximum likelihood (ML) method. These methods can be used to fit an analytical semivariogram to the experimentally obtained semivariogram. The latter is obtained by grouping the measurement points in pairs with separation distances approximating the lag distance τ. The number of pairs separated by this lag distance τ is then given by $N(\tau)$. An increase of this number generates a semivariogram that is less influenced by noisiness. The empirical semivariogram is then given by equation (4), where $x(s_i)$ resembles the measurement point at location s_i (Matheron, 1965).

$$\gamma_{exp}(\tau) = \frac{1}{2N(\tau)} \sum_{i=1}^{N(\tau)} [x(s_i + \tau) - x(s_i)]^2 \tag{4}$$

Curve fitting (CF) method

A curve fitting method, also known as least squares method (LSM), can be performed to obtain an estimation of the parameters of the chosen analytical autocorrelation function. Therefore, the parameters σ and θ are adjusted to the values $(\hat{\sigma}, \hat{\theta})$ that minimize the difference between the theoretical model and the experimental semivariogram according to equation (5).

$$(\hat{\sigma}, \hat{\theta}) = argmin\left(\boldsymbol{\gamma}_{exp} - \boldsymbol{\gamma}(\sigma, \theta)\right)^T \mathbf{C}^{-1} \left(\boldsymbol{\gamma}_{exp} - \boldsymbol{\gamma}(\sigma, \theta)\right) \tag{5}$$

Here, $\boldsymbol{\gamma}_{exp}$ and $\boldsymbol{\gamma}(\sigma, \theta)$ are the experimental and theoretical semivariogram values, respectively, and $\mathbf{C}$ is a matrix in which the elements are defined by the type of LSM used, i.e. ordinary least squares

(OLS), weighted least squares (WLS) or generalized least squares (GLS). In case of the OLS, the matrix $\mathbf{C}$ is the identity matrix; in the WLS, it is a diagonal matrix with the variances of the experimental semivariogram values on the diagonal; and in case of GLS, the matrix $\mathbf{C}$ is the covariance matrix of the semivariogram values. Traditionally, the OLS method is applied.

Maximum likelihood (ML) method

The maximum likelihood method determines values for the parameters of a model by maximising the likelihood that the process described by the model produced the data that was actually observed. Mathematically, this comes down to minimizing the negative log-likelihood function, as given by equation (6).

$$L\left(\gamma_{\exp}(\tau)\middle|\sigma,\theta\right) = \frac{n}{2}\ln(n\pi) + \frac{1}{2}\ln|\mathbf{C}| + \frac{1}{2}\left(\boldsymbol{\gamma}_{\boldsymbol{exp}}(\tau_i) - \boldsymbol{\gamma}(\sigma,\theta)\right)^T \mathbf{C}^{-1}\left(\boldsymbol{\gamma}_{\boldsymbol{exp}}(\tau_i) - \boldsymbol{\gamma}(\sigma,\theta)\right) \tag{6}$$

Here, n represents the number of lags considered in the semivariograms. Similar to the LSM, $\mathbf{C}$ is the covariance matrix of the empirical semivariogram. In the standard maximum likelihood method, this will be a diagonal matrix. Additionally, one could account for the covariance between different points of the semivariogram. A bootstrap procedure can be applied to estimate the variance-covariance matrix based on the observed experimental data.

Bootstrapping

In the curve fitting method and maximum likelihood method as described above, also the uncertainty on the empirical semivariogram and the correlation between the different points on this semivariogram can be accounted for, i.e. the covariance matrix of the empirical semivariogram can be included in the analysis. In the curve fitting method, this matrix can be accounted for by application of generalized least squares (GLS) fitting instead of ordinary least squares (OLS). In the maximum likelihood method, the matrix $\mathbf{C}$ in equation (6) can represent the covariance matrix of the empirical semivariogram.

The covariance matrix of the empirical semivariogram can be determined by application of bootstrapping. Olea & Pardo-Igúzquiza (2011) pointed out that bootstrapping the empirical semivariogram itself is incorrect as the squared differences of data pairs are not a set of independent and identically distributed data but are correlated because the data themselves correlated and because the same data appears in different pairs. Therefore, it is proposed to generate bootstrap resamples for the spatial data themselves. For this purpose, the LU decomposition can be used, as shown in (Solow, 1985; Olea & Pardo-Igúzquiza, 2011).

Estimation of scale of fluctuation: determination of sampling pattern and selection of the most robust method

General methodology

In this section, it is investigated how the sampling distance should be related to the structure length and to the scale of fluctuation in order to determine the scale of fluctuation based on the experimental results in one-dimensional elements such as beams and columns. Also, it is investigated whether one of the abovementioned methods for determination of the scale of fluctuation is more robust than the others, or whether one analytical correlation model is more stable than the others. These investigations are performed based on simulated data and the general procedure is visualized in the flowchart in Fig. 1.

First, an actual correlation model is assumed, together with a correlation length and a value for the variability of the parameter that is considered to be measured. Based on these assumptions, *N* realizations of the random field are generated. These realizations of the random field are used to generate fictitious measurements, by superimposing a measurement error and considering a sampling scheme, i.e. the distance Δx between the different measurements. By application of one of the methods described before and by assuming an analytical correlation model from Table 1, the scale of fluctuation and standard deviation of the parameter are estimated. These estimated values are indicated by $\hat{\theta}$ and $\hat{\sigma}_{par}$. Hence, for each assumption on the actual correlation model, the correlation length θ/L, the variability of the parameter σ_{par}, the sampling scheme Δx, the measurement error, estimation method and assumed analytical correlation model, *N* values of $\hat{\theta}$ and $\hat{\sigma}_{par}$ are obtained. As such, it can be assessed how well a combination of different parameters leads to an accurate estimate of the actual scale of fluctuation and variability of the parameter. A comparison is made by analysing boxplots of $\ln\left(\frac{\hat{\theta}}{\theta}\right)$ favouring a low median and interquartile range (IQR), representing a low variability of the estimate.

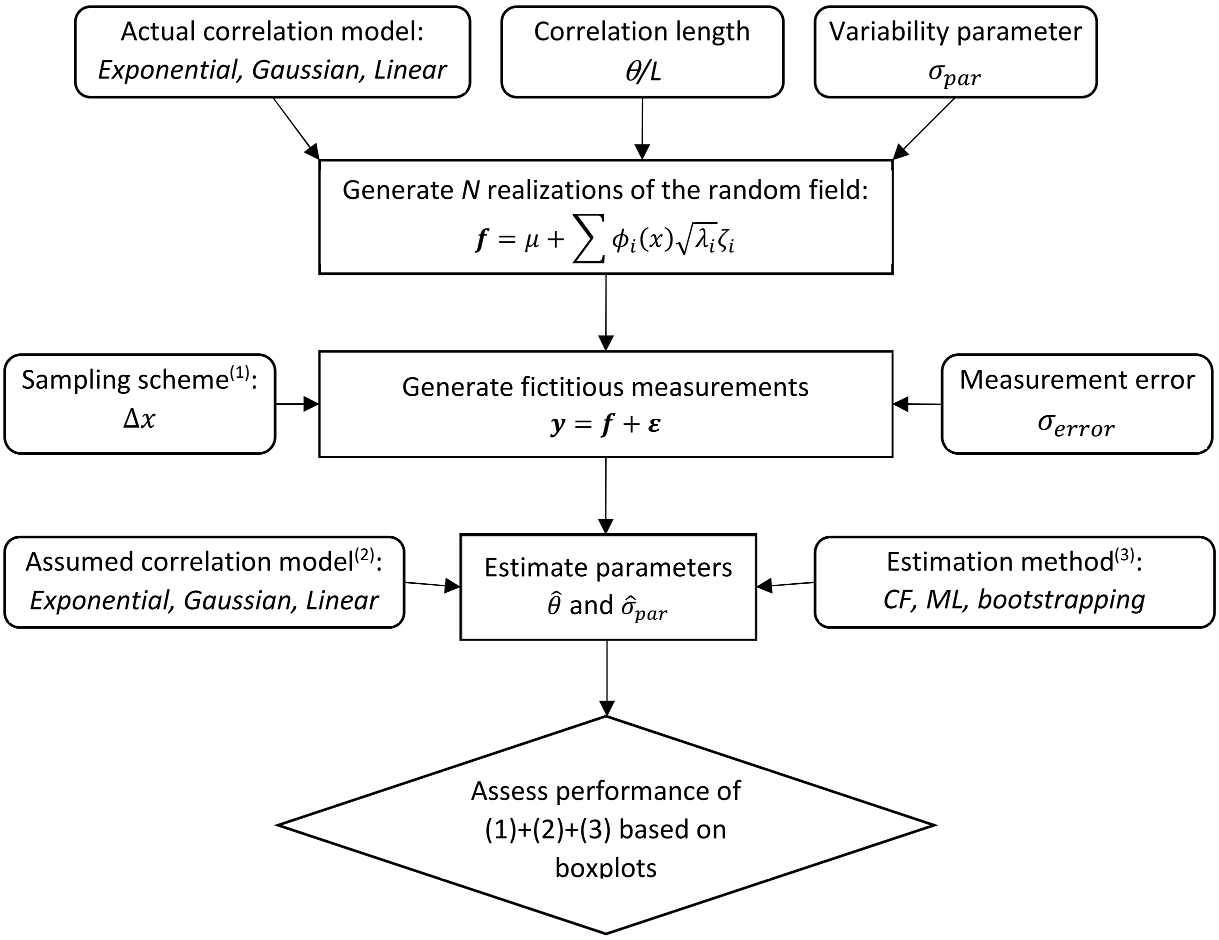

Fig. 1. Flowchart for the analyses performed in this work

For the actual correlation model, three different correlation models are considered: Gaussian, exponential and linear. For the correlation length relative to the structure length, the following values are considered: θ/L equal to 1.0, 0.5, 0.1 and 0.01. The semivariograms of these different correlation models are visualized in Fig. 2. Besides the correlation model, the random field is also defined by a mean value and a standard deviation. The mean value of the random field is assumed equal to 1 for the purpose of generality, while for the standard deviation σ_{par} a high (0.15) and low (0.05) value are considered. In a first analysis, the measurement error is neglected and hence set equal to zero. Consequently, in these first analysis, the nugget effect is neglected (c_0 = 0). The effect of the measurement error will also be investigated further in the contribution. Here, the assumed measurement errors are represented by random white noise errors, considering different values for the standard deviation of this measurement error σ_{error}: 0.01 and 0.05. Finally, for the sampling distances Δx, values of 0.001L, 0.01L and 0.1L are considered.

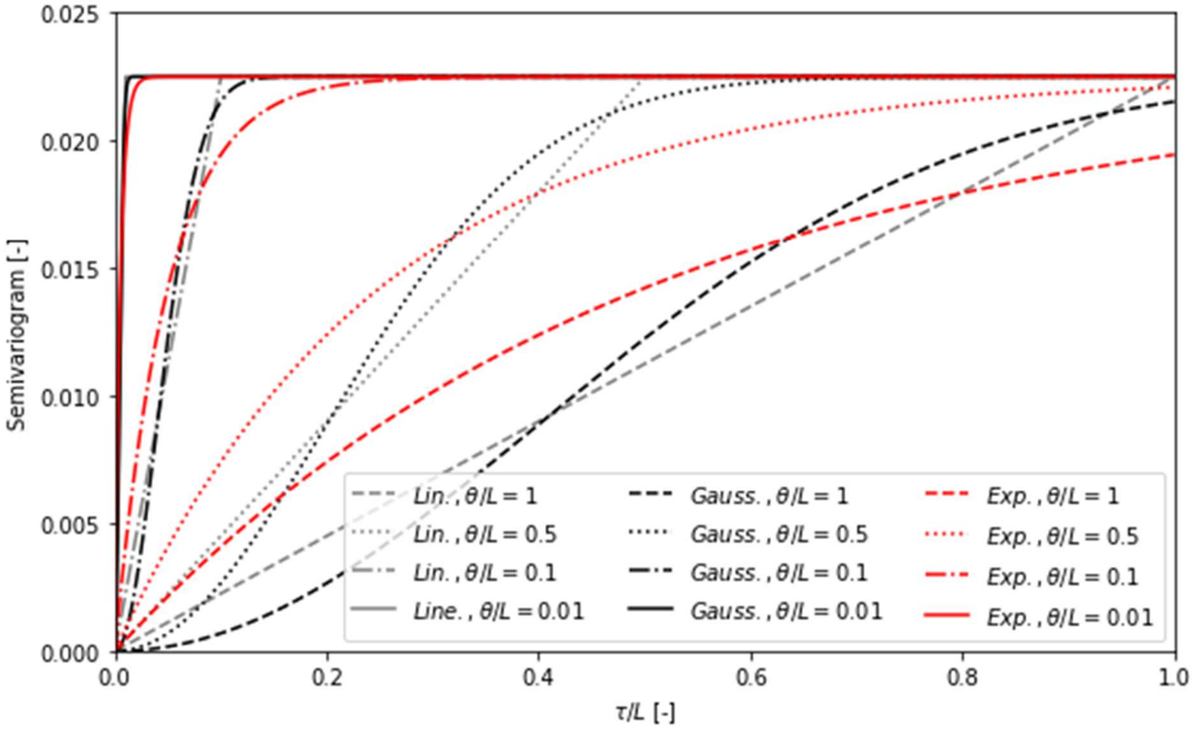

Fig. 2. Semivariograms for the different correlation models considered in this work (situation without measurement error)

Results when assuming no measurement error

The different assumptions on the analytical model, actual correlation model, sampling distance, scale of fluctuation and variability of the parameter as summarized in the previous section are considered. The influence of these different parameters on the estimate of the scale of fluctuation is investigated in order to detect whether suggestions can be provided on the most appropriate fitting method and/or the most appropriate sampling distance to experimentally determine the scale of fluctuation.

Results

For a certain combination of σ_{par}, given correlation model, scale of fluctuation, sampling distance, assumed analytical model, and one of the fitting methods, a set of estimated scales of fluctuation $\hat{\theta}$ is found. An example of the associated boxplots is given in Fig. 3, when the scale of fluctuation is determined based on the curve-fitting method (without (CF) or with (CFCOV) bootstrapping) and the maximum likelihood method (without (ML) or with (MLCOV) bootstrapping), the actual correlation model is Gaussian and the assumed analytical model is also Gaussian. The values summarized in the boxplots represent the natural logarithm of the ratio $\hat{\theta}/\theta$. The variability of the parameter σ_{par} is equal to 0.15, but similar boxplots are found for a variability of 0.05. The horizontal axis either represents the sampling distance relative to the scale of fluctuation ($\Delta x/\ \theta$ – bottom axis) or relative to the structure length ($\Delta x/L$ – top axis). The different subplots correspond to the different scales of fluctuation used to generate the measurement results. The black horizontal lines represent the situation of a perfect estimation of the actual scale of fluctuation, or $\hat{\theta} = \theta$.

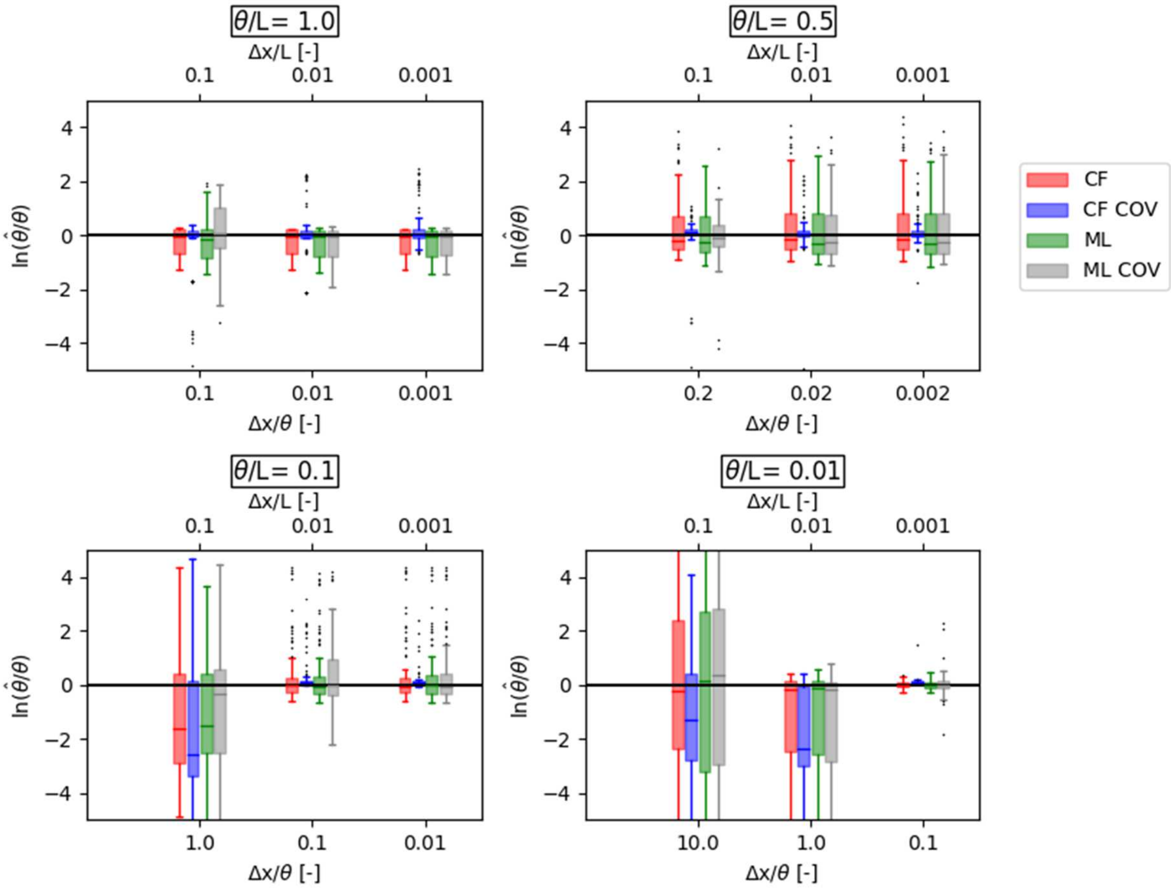

Fig. 3. Boxplots of the estimated scale of fluctuation when the actual correlation model and the analytical model are both Gaussian and the variability of the parameter is equal to 0.15

The results of the analyses are presented as a summarizing table, considering the median (*M*) and interquartile range (*IQR*) of the sets of estimations in Table 2.

For each estimation method different values for $M(\hat{\theta}/\theta)$ and $IQR(\hat{\theta}/\theta)$ are found depending on the combination of correlation models, scale of fluctuation, sampling distance, etc. Their mean values can be used in order to detect the most appropriate method. Similarly, for each considered analytical model, also different values for $M(\hat{\theta}/\theta)$ and $IQR(\hat{\theta}/\theta)$ are found, for which the mean values allow to detect the most robust analytical correlation model. Also the mean values of $M(\hat{\theta}/\theta)$ and of $IQR(\hat{\theta}/\theta)$ for the two considered values of σ_{par} are summarized.

Besides the effects of the analytical model, the variability of the parameter and the method for deriving the scale of fluctuation, there is also an influence of the sampling distance relative to the scale of fluctuation and of the scale of fluctuation relative to the length of the sampling domain. These results are shown in Table 3.

Correlation structure of empirical semivariogram

To illustrate the fact that there is indeed (significant) correlation between the different points in the empirical semivariogram, the correlation matrix for one sampled measurement result is provided in Table 4 for θ/L = 0.5 and $\Delta x/L$ = 0.1. The corresponding semivariogram is visualized in Fig. 4.

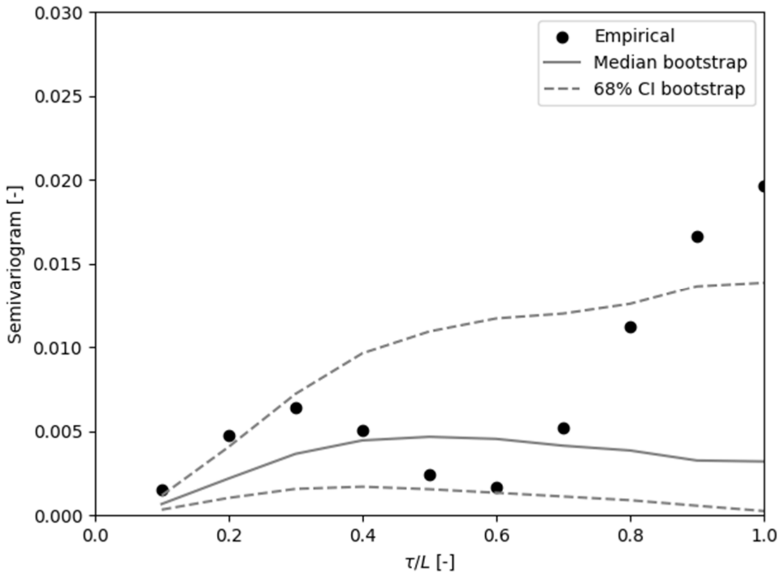

Fig. 4. Empirical semivariogram for which the correlation matrix is provided in Table 4

Discussion

When looking at Table 2, it can be seen that including the bootstrapping method in the estimation of the scale of fluctuation generally leads to a better estimation (more accurate median estimate and lower IQR). The curve fitting method also performs better than the maximum likelihood method, with a better median fit.

When considering the influence of the assumed analytical model, the best fit of the median scale of fluctuation to the actual value is found for the exponential model, closely followed by the Gaussian model. The worst fit is found for the linear model. Whereas the exponential model gives the best median fit, it leads to the largest IQR (Table 2). This IQR is smallest when assuming the Gaussian model.

Hence, overall the Gaussian model can be assumed to be the best performing and to provide the most robust estimates even if the actual correlation model is not Gaussian.

In Table 2 it can be seen that there is no clear influence of the variability of the parameter. It seems that for largest variability (σ_{par}= 0.15) the best median fit is found, whereas for the smallest variability (σ_{par}= 0.05) the lowest IQR is found.

From Table 3, it can be seen that if the sampling distance is equal to or larger than the scale of fluctuation, the median fit becomes worse and the IQR increases.

Furthermore, it can be seen that for the lowest value of the scale of fluctuation a bad median fit is found. This improves towards a maximum for a scale of fluctuation equal to 10% of the domain length *L* and then decreases again for an increase in scale of fluctuation. Similarly, the IQR is large for the smallest scale of fluctuation, then decreases to a minimum for a scale of fluctuation of 10% of the domain length *L* and then increases again for an increasing scale of fluctuation. It should be pointed out that for the lowest scale of fluctuation, the relative values of the sampling distance to the scale of fluctuation are also larger, which could be a cause of the bad estimates for this scale of fluctuation. Hence, ideally, the domain length is at least 10 times as large as the scale of fluctuation to be estimated and the sampling distances are sufficiently small (smaller than the scale of fluctuation to be estimated).

When looking at all results provided in the previous section, generally the values for $M(\hat{\theta}/\theta)$ are negative and hence an underestimation of the scale of fluctuation is found.

To conclude, there seems to be a benefit of including correlation of the semivariogram by the bootstrapping method. Moreover, the curve fitting method seems to perform better than the maximum likelihood method. When an analytical correlation model is to be chosen, the Gaussian model seems the most robust choice. There is no substantial influence of the variability of the parameter. The sampling distance needs to be smaller than the scale of fluctuation to be estimated and the domain length is ideally at least 10 times as large as this scale of fluctuation. If these criteria cannot be met, generally an underestimation of the scale of fluctuation will be found. Finally, it is important to note that for all combinations that have been assessed a significant scatter of the estimations is found (reflected by relatively large IQR values). This explains the variability of values reported in literature and also shows the possible benefit of the application of Bayesian updating techniques in which prior information regarding the spatial variability can be updated based on in situ measurements (Criel et al., 2004).

Influence of a measurement error

The influence of the presence of a measurement error is investigated in this section. A measurement error can be accounted for by means of the nugget effect in the semivariogram, i.e. the semivariogram is not equal to zero for zero lag, but will have a specific value, called the nugget c_0. To the knowledge of the authors, this effect has not been considered in scientific literature related to spatial variability in concrete structures.

In this section, the actual model to simulate the measurement results is assumed to be the Gaussian model. The assumed measurement errors are represented by random white noise, considering two different values for the standard deviation of this measurement error σ_{error}: 0.01 and 0.05.

The analytical model to fit the semivariogram to the empirical one is assumed Gaussian, corresponding to the conclusions of the previous section. The sampling distance is taken sufficiently small compared to the scale of fluctuation, i.e. $\Delta x/\theta$ is chosen equal to 0.1. Two values for the scale of fluctuation are considered, i.e. θ/L equal to 0.1 and 1. The curve fitting method (with and without bootstrapping) will be used to estimate the scale of fluctuation. When applying the curve fitting method, two situations are investigated. In the first situation, the nugget effect is neglected, i.e. $c_0 = 0$ corresponding to current practice. In the second situation, the nugget c_0 is estimated based on the curve fitting method, together with the scale of fluctuation θ and the variability of the parameter σ_{par}.

The results of these investigations are illustrated in Fig. 5 and Fig. 6, considering $\sigma_{par} = 0.05$ and $\sigma_{par} = 0.15$ respectively. Here, 'CF nugget' indicates that the curve fitting method is applied and that the nugget c_0 is also estimated. When looking at Fig. 5 and Fig. 6, it can be seen that in case of the presence of a measurement error, the curve fitting method combined with bootstrapping still performs better than the ordinary curve fitting method in most of the situations. Furthermore, also estimating the nugget provides a better fit to the actual scale of fluctuation when looking at the median of the boxplot. The larger the measurement error σ_{error}, the larger the benefit of also estimating the nugget effect. If the nugget effect is neglected for the larger measurement errors, the median of the boxplot deviates significantly from the actual value. This is more pronounced for $\sigma_{par} = \sigma_{error} = 0.05$ due to the large measurement error compared to the variability of the parameter. The estimate of the scale of fluctuation is also better for a lower ratio of θ/L, which could be expected beforehand based on the results in the previous section. Finally, the IQR's are also larger than for the situation where no measurement errors are considered (see Fig. 3) and as also found in the previous section, generally the median of the boxplots tends to underestimate the actual scale of fluctuation if the experimental parameters are chosen inappropriate.

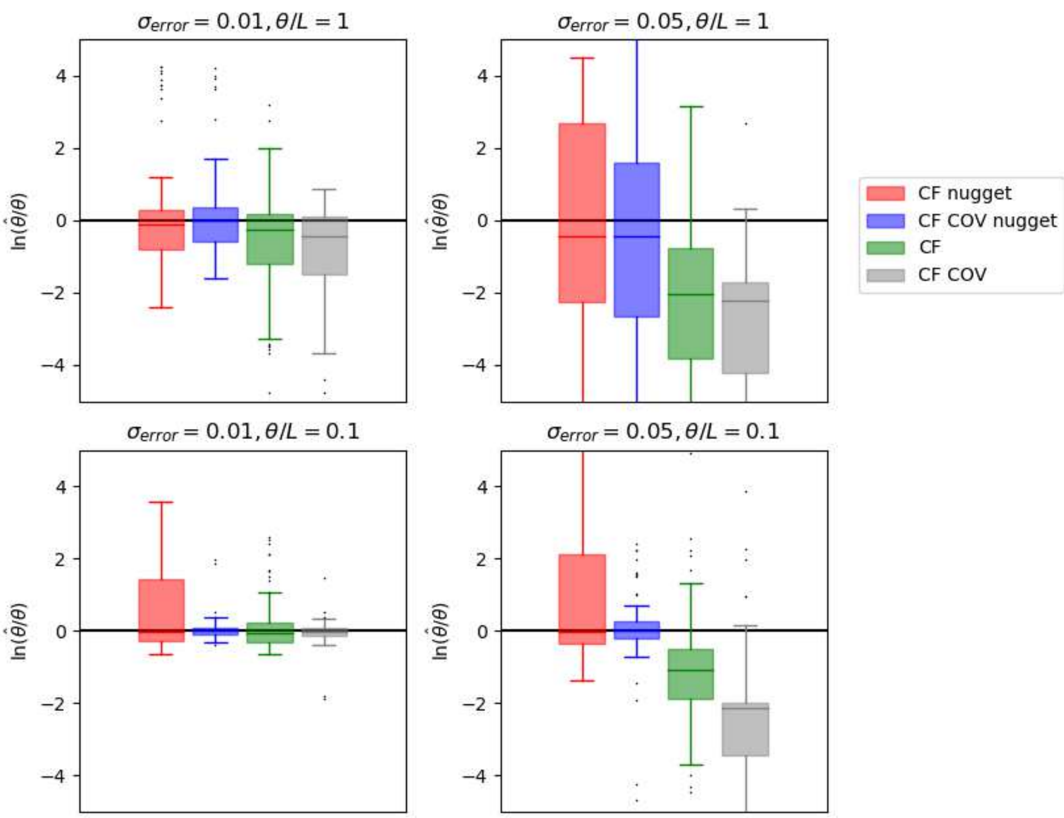

Fig. 5. Results of investigations with a measurement error with $\sigma_{par} = 0.05$

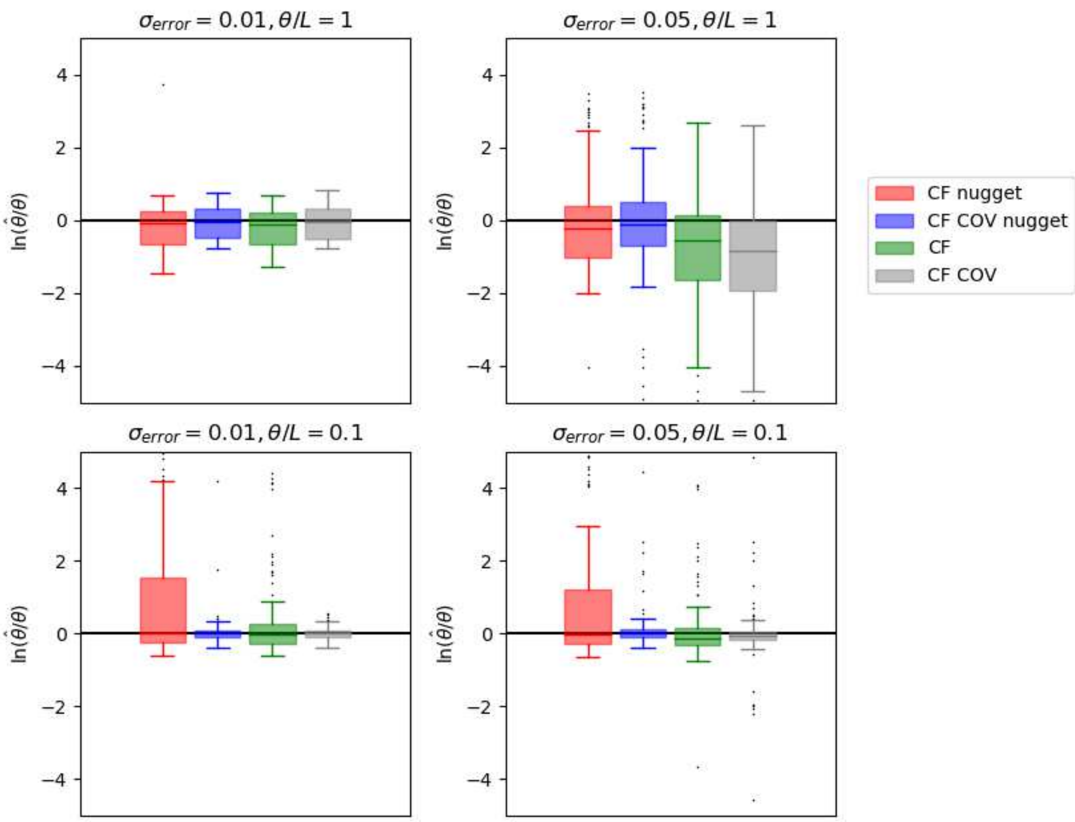

Fig. 6. Results of investigations with a measurement error with $\sigma_{par} = 0.15$

Application example: experimental investigation of spatial variability in reinforced concrete

In this section, the correlation length is determined based on experimental investigations on a reinforced concrete beam. Different mechanical properties of concrete (compressive strength, tensile strength and diffusion coefficient) have been determined based on drilled cores taken from the beam. The correlation model and correlation length for these different material properties are determined based on the different estimation methods described before. Furthermore, four other beams have been subjected to accelerated corrosion. Also this data is used to estimate the scale of fluctuation corresponding to the corrosion process.

Description of the experimental campaign

The beams under investigation are reinforced concrete beams of 5 m long, with a height of 400 mm and a width of 300 mm. The reinforcement layout of the beams is illustrated in Fig. 7 and 8.

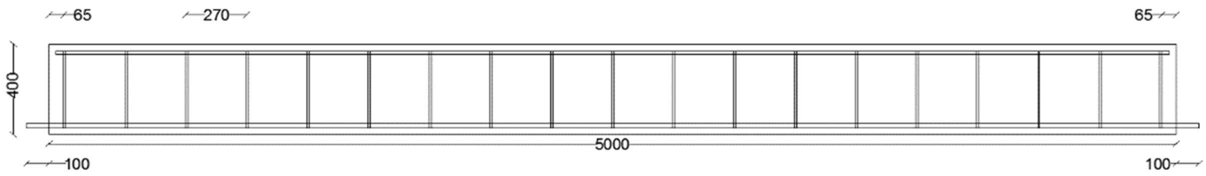

Fig. 7. Longitudinal section of the beams (dimensions in mm)

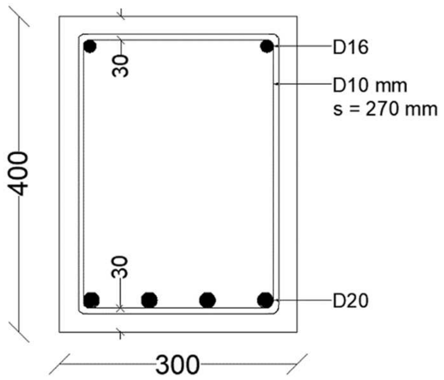

Fig. 8. Cross-section of the beams (dimensions in mm)

The concrete used for the beams has a composition according to Table 5. The concrete has chloride class 0.4%, environment class EI, maximum aggregate size D_{max}= 14 mm, consistency class S4 and strength class C25/30.

At a concrete age of 65 days, cores were drilled horizontally from one of the beams, through the entire thickness of the beam, resulting in cores with a height of 300 mm. The diameter of these cores was 100 mm. Furthermore, these cores were taken in between the stirrups, with two cores in between each pair of stirrups. The cores were taken at 140 mm from the bottom edge and the spacing between two consecutive cores equals 135 mm. After drilling, the cores were cut in three slices, which were subsequently used to determine the compressive strength, tensile strength and diffusion coefficient.

The concrete compressive strength was tested according to NBN EN 12390-3 (CEN, 2019), the concrete tensile strength was tested according to NBN EN 12390-6 (CEN, 2005), and the diffusion coefficient was determined based on a rapid chloride migration test as described in (NORDTEST, 1999). The resulting data sets are the following:

- 36 test results for concrete compressive strength (on 36 locations along the beam, spacing 135 mm);
- 18 test results for concrete tensile strength (on 18 locations along the beam, spacing 270 mm);
- 18 test results for the rapid chloride migration test (on 18 locations along the beam, spacing 270 mm).

Here, these data sets are used to determine the correlation model for the concrete compressive strength, the concrete tensile strength and the diffusion coefficient of the concrete.

The remaining four beams (indicated as ‘B’, ‘C’, ‘D’ and ‘E’) were subjected to accelerated corrosion. Therefore, an imposed current of 100 $\mu A/cm^2$ was applied to the reinforcement, whereas a stainless steel plate submerged in a 5% NaCl solution was used as cathode. After reaching a certain target corrosion degree between 2% and 30%, the reinforcement was removed from the beam and cut into pieces of 200 mm. Next, these pieces were cleaned and weighed, to determine the mass loss due to corrosion. The resulting data sets are used to determine the correlation model for the corrosion degree in this work. More details regarding the accelerated corrosion tests can be found in (Vereecken, 2022).

Empirical semivariograms and bootstrapping

In this section, based on the different datasets, the empirical semivariograms are derived. It was found previously that bootstrapping can be used to, among others, determine the variance-covariance matrix of the points in the semivariogram. Additionally, the results of such bootstrapping procedure also allows estimating the average semivariogram as well as uncertainty bounds based on the experimentally observed data. Such an approach is deemed extremely useful since experimental semivariograms that are determined based on limited data (which is often the case for destructive tests on concrete) can be significantly affected by outliers. Due to the bootstrapping procedure the effect of these outliers on the semivariogram can be reduced.

From the M (= 2000) bootstrapping resamples, the median semivariogram is evaluated as well as the 68% confidence interval (CI) according to (Olea & Pardo-Igúzquiza, 2011). These results are visualized in Fig. 9. In case of the corrosion degree, the considered experimental results are normalized by considering the measured corrosion degrees divided by the average corrosion degree over the length of the beam. As such, the corrosion degrees of the four beams subjected to accelerated corrosion can be compared amongst each other. Furthermore, such normalization does not influence the estimation of the scale of fluctuation.

In general, Fig. 9 shows that the uncertainty related to the semivariogram values increases for larger lag distances. This can be attributed to the fact that for these larger lag distances less data is available. Furthermore, the typical trend for a semivariogram is more apparent for the derived median of the semivariogram than for the experimentally observed semivariogram.

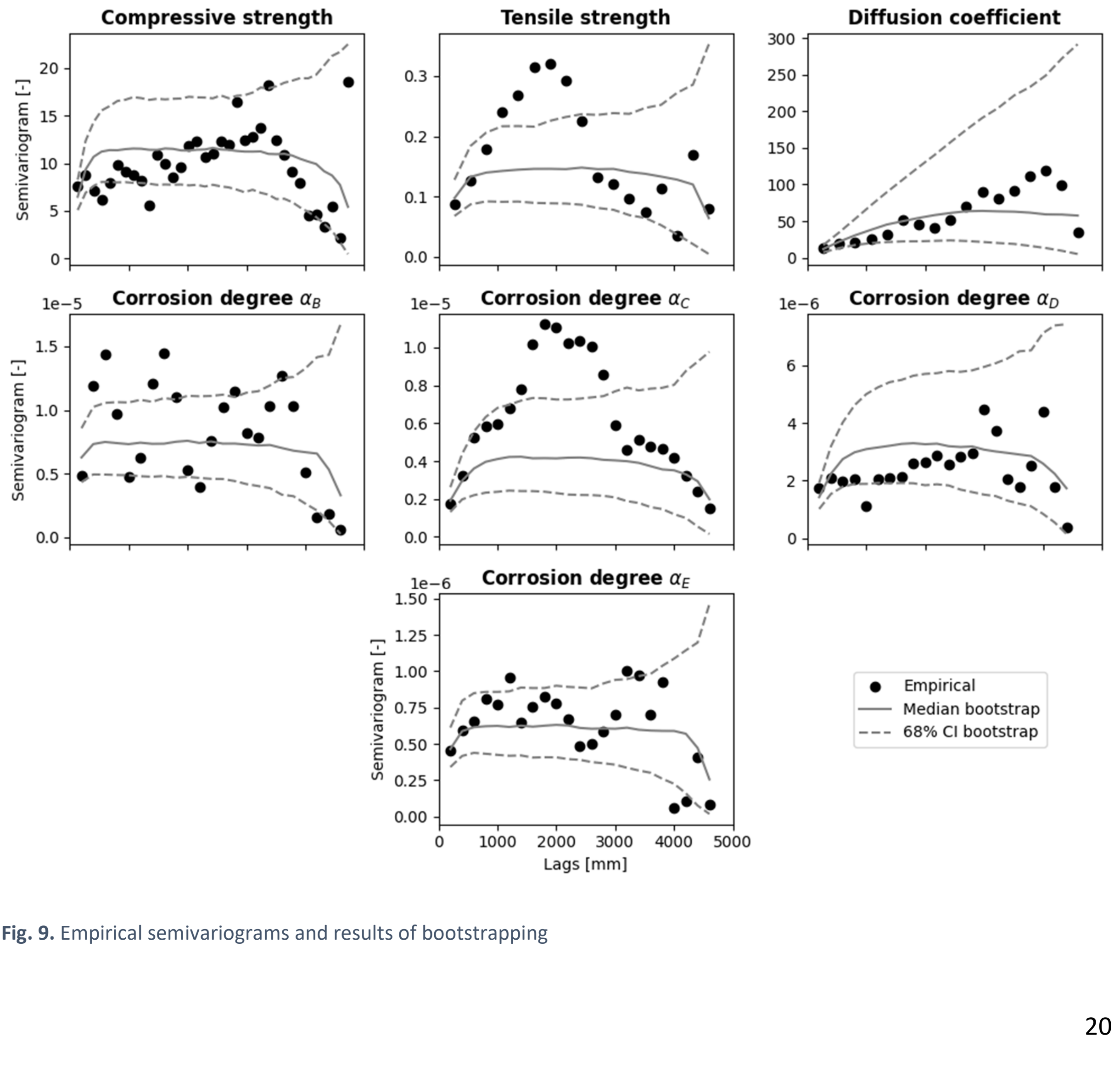

Fig. 9. Empirical semivariograms and results of bootstrapping

Determination of the correlation model

Next, the correlation model is estimated based on the experimental data. For this purpose, the curve fitting method will be applied since this was found to provide better results compared to the maximum likelihood method. The three different analytical models are considered, and each time the nugget is once estimated and once neglected. The most appropriate model is selected as the one providing the best fit to the experimental semivariogram, i.e. the one with the lowest least-squares value. For each variable, the selected correlation model, scale of fluctuation, variability of the parameter and nugget are summarized in Table 6.

It can be seen that for the concrete properties, generally a linear correlation model provides the best fit, and that a nugget effect is present. Especially in case of the compressive strength, the latter effect seems to be significant, indicating a relatively large measurement error possibly induced by drilling the cores. The scale of fluctuation differs between the different properties, with a scale of fluctuation of 813 mm for the concrete tensile strength, 2160 mm for the concrete compressive strength and 3605 mm for the diffusion coefficient of the concrete. These values are in the same order of magnitude as often suggested in literature based on engineering judgement, see e.g. (Straub, 2011; Tran et al., 2012; Hajializadeh et al., 2016). In literature, the linear correlation model is not selected. Nevertheless, for the investigated experimental results, the fit when assuming a Gaussian correlation model is almost equally good as for a linear correlation model. Furthermore, the corresponding estimates of the nugget, variance of the parameter and scale of fluctuation are almost unaffected when changing from a linear to a Gaussian correlation model. The corresponding results are provided in Table 7.

Apart from estimating the covariance matrix, the bootstrapping procedure also allows to assess the uncertainties related to the estimated parameters by fitting a semivariogram to each bootstrapped semivariogram. The results are provided for the concrete properties in Table 7 in terms of the median estimate as well as the first and third quartile, assuming a Gaussian model for each fit. As expected from the theoretical investigations (cfr. supra), a relatively large scatter of the scale of fluctuation is observed. Furthermore, it is clear that the median estimate of this parameter obtained by bootstrapping is not necessarily close to the value obtained from fitting the experimental results.

For the corrosion degrees, generally the Gaussian model provides the best fit. For this situation, the nugget effect was neglected as no large measurement error was expected due to the non-destructive nature of the measurements. For most beams, the variability of the parameter $\hat{\sigma}_{par}$ is about the same, and lies around 0.0025. The scales of fluctuation for the corrosion degrees are all of the same order of magnitude, ranging from 327 mm to 879 mm if the Gaussian correlation model and no nugget effect are assumed. It should be pointed out that these correlation lengths for the corrosion degree are in contrast to the results provided in (Zhou et al., 2022) where no correlation for the corrosion degree was found. Nevertheless, the latter research was based on bars with a length of 500 mm cut in pieces of 20 mm. This bar length of 500 mm is smaller than the correlation length found for the corrosion degree in the current work, and could hence not detect these larger correlation lengths, which was acknowledged by the authors in their conclusions.

It was observed that when considering the nugget effect in the estimation for the corrosion degrees, this could result in significantly different estimated scales of fluctuation, e.g. 2200 mm in case of beam D. For the latter case, the nugget effect ($\hat{c}_0 = 1.24e - 6$) was estimated to be (significantly) higher than the variance ($\hat{\sigma}_{par}^2 = 1.08e - 6$) and, consequently, a semivariogram with a longer scale of fluctuation better fits the data. Therefore, it seems important to carefully consider whether or not a (significant) nugget effect is to be expected and taken along in the estimation process.

Discussion

When considering the experimental results, there are some links to be made with the analytical results from the previous section. Overall, the Gaussian correlation model provides a good fit to the data. Also in the theoretical analyses it was found that generally the Gaussian correlation model is a robust choice for the analytical correlation model. Further, the theoretical analyses showed that there is a benefit of applying the bootstrapping method and including correlation between the points of the empirical semivariogram in the analyses. This also shown in the plots in Fig. 9, where the median of the bootstrapping method indeed better approximates a semivariogram that could be represented by one of the assumed analytical correlation models.

According to the theoretical analysis (cfr. supra), the sampling distance needs to be smaller than the scale of fluctuation. This is indeed the case for the results summarized in the previous section. Consequently also the effect of the different sampling distance for the compressive strength compared to the tensile strength and diffusion coefficient is expected to be very limited.

From the theoretical analyses, the ideal ratio between the scale of fluctuation and the sampling domain was equal to 0.1, in this case leading to a scale of fluctuation of 500 mm. Nevertheless, most estimates of the scale of fluctuation in the analysis above are larger than 500 mm. Hence, the estimates found for the scale of fluctuation might underestimate the actual scale of fluctuation. The estimated scale of fluctuation is largest for the diffusion coefficient and close to the length of the beam (5000 mm). Hence, there might be some uncertainty on this estimate, which is reflected by the large interquartile interval for this parameter. Finally, for all concrete parameters also including the nugget effect in the estimate led to the best fit. This is in correspondence with the observations from the theoretical investigations presented before.

Conclusions

The authors investigated the effect of several parameters and choices to be made by an engineer in deriving the correlation model based on experimental data from destructive tests. The influence of different parameters in the experimental program were investigated, such as the sampling distance, the size of the sampling domain compared to the scale of fluctuation and the measurement error. Also the influence of assumptions that need to be made when fitting the correlation model to the experimental data has been studied, including the choice of the analytical correlation model and the method applied to perform the fit.

Different methods for deriving the scale of fluctuation were selected and compared, i.e. the curve fitting method and the maximum likelihood method, with or without the consideration of correlation by application of bootstrapping. It has been illustrated that the curve fitting method generally leads to better estimates of the scale of fluctuation compared to the maximum likelihood method. Moreover, there is a clear benefit of applying the bootstrapping procedure to the experimental data.

Also the influence of the selected analytical correlation model has been investigated, and here the Gaussian model was found to be the most robust choice, even if the actual correlation model is not Gaussian.

Considering the design of an experimental program, it was found that the sampling distance needs to be small with respect to the scale of fluctuation to be estimated and that the size of the sampling domain needs to be at least 10 times larger than the actual scale of fluctuation. If these criteria are not met, generally an underestimation of the scale of fluctuation is found.

If there are no measurement errors, there is almost no influence of the variability of the measured parameter on the estimate of the scale of fluctuation. This variability becomes more important if also measurement errors are present: if the measurement error becomes large with respect to the variability of the measured parameter, this leads to an increased deviation between the actual scale of fluctuation and the estimated scale of fluctuation, especially if the nugget effect is neglected. Hence, when a measurement error is suspected to be present and cannot be neglected, the nugget should be estimated together with the variance and the scale of fluctuation.

The findings from the numerical analyses were subsequently applied to actual experimental data on the material properties of concrete, i.e. data related to the concrete tensile strength, compressive strength and diffusion coefficient. Also the spatial variability of the corrosion degree obtained in accelerated corrosion tests was investigated. It was found that a Gaussian model provided a good fit to the data in all cases, which is in line with the findings from the numerical analyses which indicated that this model is the most robust. Furthermore, including the nugget effect led to a better fit of the experimentally obtained semivariogram of the concrete properties. The latter indicate the presence of an important uncertainty introduced by destructive testing of specimens (e.g. drilling of cores). In case of non-destructive testing (determination of the corrosion degree of corroded reinforcement), it was found that including the nugget effect in the estimation process could result in significantly different results. Therefore, the parameters to be estimated should be chosen with care.

Finally, the estimated scales of fluctuation were in line with those currently found in literature, which are based on engineering judgement. Apart from a median estimate of the scale of fluctuation, also the uncertainty of this estimate could be obtained in case a bootstrapping procedure is adopted. The latter uncertainties were shown to be significant, implying the importance of assessing the sensitivity of the behaviour of the element under consideration to spatial variability. In case of elements sensitive to spatial variations, one might consider to update the model describing the spatial variability by means of e.g. Bayesian updating (Criel et al., 2004), where the prior information can be adopted from this research.

Data Availability Statement

Some or all data, models, or code that support the findings of this study are available from the corresponding author upon reasonable request.

Acknowledgements

This research has been made possible through funding from the Research Foundation Flanders (FWO) under grant numbers G013317N (Eline Vereecken), 12X1719N and S001021N (Wouter Botte), for which FWO is gratefully acknowledged.

References

Cami, B., Javankhoshdel, S., Phoon, K. K., & Ching, J. (2020). Scale of fluctuation for spatially varying soils: estimation methods and values. ASCE-ASME Journal of Risk and Uncertainty in Engineering Systems, Part A: Civil Engineering, 6(4), 03120002.

CEN. (2005). NBN EN 12390-6 Testing hardened concrete - Part 6: Tensile splitting strength of test specimens.

CEN. (2019). NBN EN 12390-3:2019 Testing hardened concrete - Part 3: Compressive strength of test specimens.

Chen, J., He, J., Ren, X., & Li, J. (2018). Stochastic harmonic function representation of random fields for material properties of structures. Journal of Engineering Mechanics, 144(7), 04018049. https://doi.org/10.1061/(ASCE)EM.1943-7889.0001469

Christodoulou, P., Pantelidis, L., & Gravanis, E. (2021). A Comparative Assessment of the Methods-of-Moments for Estimating the Correlation Length of One-Dimensional Random Fields. Archives of Computational Methods in Engineering, 28(3), 1163–1181. https://doi.org/10.1007/s11831-020-09408-2

Criel, P., Caspeele, R., & Taerwe, L. (2014). Bayesian updated correlation length of spatial concrete properties using limited data. Computers and Concrete, 13(5), 659–677. https://doi.org/10.12989/cac.2014.13.5.659

Duprat, F. (2007). Reliability of RC beams under chloride-ingress. Construction and Building Materials, 21(8), 1605–1616.

Engelund, S. (1997). Probabilistic Models and Computational Methods for Chloride Ingress in Concrete. Aalborg University, Aalborg.

Feng, D. C., Liang, Y. P., Ren, X., & Li, J. (2022). Random fields representation over manifolds via isometric feature mapping-based dimension reduction. Computer-Aided Civil and Infrastructure Engineering, 37(5), 593-611. https://doi.org/10.1111/mice.12752

Hajializadeh, D., Stewart, M. G., Enright, B., & OBrien, E. (2016). Spatial time-dependent reliability analysis of reinforced concrete slab bridges subject to realistic traffic loading. Structure and Infrastructure Engineering, 12(9), 1137–1152. https://doi.org/10.1080/15732479.2015.1086385

He, J., Chen, J., Ren, X., & Li, J. (2021). Uncertainty quantification of random fields based on spatially sparse data by synthesizing Bayesian compressive sensing and stochastic harmonic function. Mechanical Systems and Signal Processing, 153, 107377. https://doi.org/10.1016/j.ymssp.2020.107377

He, J., Gao, R., & Chen, J. (2022). A sparse data-driven stochastic damage model for seismic reliability assessment of reinforced concrete structures. Reliability Engineering & System Safety, 223, 108510. https://doi.org/10.1016/j.ress.2022.108510

Journel, A. G., & Huijbregts, C. J. (1978). Mining Geostatistics. London, England: Academic Press.

Li, Y., Vrouwenvelder, T., Wijnants, G. H., & Walraven, J. (2004). Effect of Spatial Variability on Maintenance and Repair Decisions for Concrete Structures. Structural Concrete, 5(3), 121–129.

Liang, Y. P., Ren, X., & Feng, D. C. (2022). Efficient stochastic finite element analysis of irregular wall structures with inelastic random field properties over manifold. Computational Mechanics, 1-17. https://doi.org/10.1007/s00466-021-02084-4

Matheron, G. (1965). Les Variables Regionalisees et leur Estimation. Paris: Masson.

NORDTEST. (1999). NT BUILD 492 Concrete, mortar and cement-based repair materials: Chloride migration coefficient from non-steady-state migration experiments.

O'Connor, A., & Kenshel, O. (2013). Experimental Evaluation of the Scale of Fluctuation for Spatial Variability Modeling of Chloride-Induced Reinforced Concrete Corrosion. Journal of Bridge Engineering, 18(1), 3–14. https://doi.org/10.1061/(ASCE)BE.1943-5592.0000370

Olea, R. A., & Pardo-Igúzquiza, E. (2011). Generalized Bootstrap Method for Assessment of Uncertainty in Semivariogram Inference. Mathematical Geosciences, 43(2), 203–228. https://doi.org/10.1007/s11004-010-9269-6

Solow, A. R. (1985). Bootstrapping correlated data. Journal of the International Association for Mathematical Geology, 17(7), 769–775. https://doi.org/10.1007/BF01031616

Stewart, M. G., & Mullard, J. A. (2007). Spatial time-dependent reliability analysis of corrosion damage and the timing of first repair for RC structures. Engineering Structures, 29(7), 1457–1464. https://doi.org/10.1016/j.engstruct.2006.09.004

Straub, D. (2011). Reliability updating with inspection and monitoring data in deteriorating reinforced concrete slabs. ICASP11 - Applications of Statistics and Probability in Civil Engineering, 2309–2316. https://doi.org/10.1201/b11332-340

Straub, D., Malioka, V., & Faber, M. H. (2009). A framework for the asset integrity management of large deteriorating concrete structures. Structure and Infrastructure Engineering, 5(3), 199–213. https://doi.org/10.1080/15732470601017369

Tomizawa, Y., & Yoshida, I. (2022). Benchmarking of Gaussian Process Regression with Multiple Random Fields for Spatial Variability Estimation. ASCE-ASME Journal of Risk and Uncertainty in Engineering Systems, Part A: Civil Engineering, 8(4), 04022052.

Tran, T. V., Bastidas-Arteaga, E., Schoefs, F., Bonnet, S., O'Connor, A. J., & Lanata, F. (2012). Structural reliability analysis of deteriorating RC bridges considering spatial variability. Bridge Maintenance, Safety, Management, Resilience and Sustainability - Proceedings of the Sixth International Conference on Bridge Maintenance, Safety and Management, (July), 698–705. https://doi.org/10.1201/b12352-94

Vanmarcke, E. (2010). Random Fields Analysis and Synthesis. World Scientific.

Vanmarcke, E. H. (1977). Probabilistic Modeling of Soil Profiles. ASCE J Geotech Eng Div, 103(11), 1227–1246. https://doi.org/10.1061/ajgeb6.0000517

Vereecken, E. (2022). Applied Bayesian pre-posterior and life-cycle cost analysis for determining and optimizing the value of structural health monitoring for concrete structures. Ghent University. Faculty of Engineering and Architecture, Ghent, Belgium.

Vu, K. A., & Stewart, M. G. (2005). Predicting the Likelihood and Extent of Reinforced Concrete Corrosion-Induced Cracking. Journal of Structural Engineering, 131(11), 1681–1689. https://doi.org/10.1061/(asce)0733-9445(2005)131:11(1681)

Vu, K. A. T. (2003). Corrosion-induced cracking and spatial timedependent reliability analysis of reinforced concrete structures. The University of Newcastle, New South Wales, Australia.

Webster, R., & Oliver, M. A. (1992). Sample adequately to estimate variograms for soil properties. J. Soil Sci., 43, 177–192.

Hu, Y., Wang, Y., Zhao, T., & Phoon, K. K. (2020). Bayesian supervised learning of site-specific geotechnical spatial variability from sparse measurements. ASCE-ASME Journal of Risk and Uncertainty in Engineering Systems, Part A: Civil Engineering, 6(2), 04020019.

Zhao, T., & Wang, Y. (2020). Non-parametric simulation of non-stationary non-gaussian 3D random field samples directly from sparse measurements using signal decomposition and Markov Chain Monte Carlo (MCMC) simulation. Reliability Engineering & System Safety, 203, 107087. https://doi.org/10.1016/j.ress.2020.107087

Zheng, L., & Silliman, S. E. (2000). Estimating the theoretical semivariogram from finite numbers of measurements. Water Resources Research, 36(1), 361–366. https://doi.org/10.1029/1999WR900270

Zhou, H., Li, Y., Wen, Q., & Deodatis, G. (2022). Stochastic field model for the residual radius along the length of naturally and artificially corroded rebars. Structure and Infrastructure Engineering, https://doi.org/10.1080/15732479.2022.2027471

Tables

Table 1. Summary of covariance functions and corresponding semivariograms used in this work

Name	Covariance function $B(\tau)$	Semivariogram $\gamma(\tau)$	$\theta(\rho_l)$
Exponential	$\sigma^2 \exp\left(-\frac{\lvert\tau\rvert}{\frac{\theta}{2}}\right)$	$c_0 + \sigma^2\left(1 - \exp\left(-\frac{\lvert\tau\rvert}{\frac{\theta}{2}}\right)\right)$	$2\rho_l$
Gaussian	$\sigma^2 \exp\left(-\frac{\lvert\tau\rvert^2}{\left(\frac{\theta}{\sqrt{\pi}}\right)^2}\right)$	$c_0 + \sigma^2\left(1 - \exp\left(-\frac{\lvert\tau\rvert^2}{\left(\frac{\theta}{\sqrt{\pi}}\right)^2}\right)\right)$	$\rho_l\sqrt{\pi}$
Linear	$\begin{cases} \sigma^2\left(1 - \frac{\tau}{\theta}\right) & \tau < \theta \\ 0 & otherwise \end{cases}$	$\begin{cases} c_0 + \sigma^2\left(\frac{\tau}{\theta}\right) & \tau < \theta \\ c_0 + \sigma^2 & otherwise \end{cases}$	ρ_l

Table 2. Influence of the method used for parameter estimation and of the assumed analytical model on the estimated scale of fluctuation

σ_{par}	Analytical model	*Method for parameter estimation*									
		CF		*CFCOV*		*ML*		*MLCOV*		*(1)*	
		M	IQR	M	IQR	M	IQR	M	IQR	M	IQR
0.15	Exponential	0.1	3.5	1.5	2.5	-0.9	4.9	0.5	4.5	0.3	3.8
	Gaussian	-0.2	1.6	-1.4	1.7	-0.2	1.8	-0.5	1.9	-0.5	1.7
	Linear	-0.8	1.4	-0.3	2.3	-1.0	1.5	-1.0	1.7	-0.7	1.7
	(2)	-0.3	2.2	0.0	2.2	-0.7	2.7	-0.3	2.7	-0.3	2.4
0.05	Exponential	0.3	3.8	1.6	2.8	-0.2	2.3	-0.2	2.2	0.4	2.8
	Gaussian	-0.2	1.6	-1.0	1.6	-0.4	1.7	-0.6	1.9	-0.6	1.7
	Linear	-0.8	1.4	-0.3	2.3	-1.0	1.6	-1.1	1.9	-0.8	1.8
	(2)	-0.2	2.3	0.1	2.2	-0.6	1.8	-0.6	2.0	-0.3	2.1

(1) Average over the different estimation methods

(2) Average over the different analytical models

Table 3. Influence of the sampling distance and the actual scale of fluctuation on the estimated scale of fluctuation

$\Delta x/\theta$	M	IQR
0.001	-0.1	1.6
0.002	-0.3	1.5
0.01	-0.1	1.2
0.02	-0.3	1.6
0.1	-0.0	1.0
0.2	-0.3	1.6
1	-0.6	2.9
10	-1.4	4.8

θ/L	M	IQR
0.01	-0.6	2.5
0.1	-0.2	1.2
0.5	-0.3	1.5
1	-0.4	1.7

Table 4. Example of a correlation matrix between the points of an empirical semivariogram derived based on bootstrapping (symmetric matrix – only lower triangle values are presented)

$\hat{\gamma}(d_k)$	*k* = 1	*k* = 2	*k* = 3	*k* = 4	*k* = 5	*k* = 6	*k* = 7	*k* = 8	*k* = 9	*k* = 10
k = 1	1.00									
k = 2	0.99	1.00								
k = 3	0.93	0.98	1.00							
k = 4	0.83	0.89	0.97	1.00						
k = 5	0.68	0.75	0.86	0.96	1.00					
k = 6	0.50	0.57	0.68	0.81	0.94	1.00				
k = 7	0.32	0.38	0.47	0.61	0.79	0.94	1.00			
k = 8	0.20	0.24	0.32	0.45	0.61	0.80	0.94	1.00		
k = 9	0.14	0.17	0.24	0.33	0.45	0.61	0.80	0.94	1.00	
k = 10	0.13	0.16	0.19	0.23	0.31	0.42	0.58	0.78	0.93	1.00

Table 5. Concrete composition

Component	**Content [kg/m³]**
K 6.3/14 (limestone 6.3/14 Benor Holcim)	955
Sea sand	518
K 0/4 (washed limestone sand Holcim Gaurain Benor)	427
CEM I 52.5 N Holcim	270
Water	174 (183 incl. absorption water)
Superplasticizer Sky 571 (BASF)	1.9

Table 6. Results of the fits to the experimental data

Variable		**Model**	$\hat{\theta}$ **[mm]**	$\hat{\sigma}_{par}^{2}$	$\hat{c}_0$
Concrete tensile strength	f_{ct}	Linear	813	0.14 MPa²	0.04 MPa²
Concrete compressive strength	f_c	Linear	2160	3.57 MPa²	6.92 MPa²
Diffusion coefficient	D	Linear	3605	89.11 (mm²/yr.)²	1.96 (mm²/yr.)²
Corrosion degree beam B	α_B	Gaussian	352	8.62e-6	0
Corrosion degree beam C	α_C	Gaussian	879	6.77e-6	0
Corrosion degree beam D	α_D	Gaussian	327	2.44e-6	0
Corrosion degree beam E	α_E	Gaussian	339	6.55e-7	0

Table 7. Results of the fits to the experimental data for the concrete properties and uncertainty assessment based on bootstrapping procedure when assuming a Gaussian correlation model

	θ			σ_{par}^2			c_0		
Var.	**Exp.**	M	[Q1; Q3]	**Exp.**	M	[Q1; Q3]	**Exp.**	M	[Q1; Q3]
f_{ct}	856	760	[385; 3292]	0.13	0.13	[0.07; 0.19]	0.05	0.05	[0.00; 0.10]
f_c	2288	507	[279; 2218]	3.20	8.72	[5.70; 12.41]	7.25	4.61	[0.98; 6.82]
D	4155	2763	[1182; 7664]	82.63	89.25	[34.43; 513.48]	1.96	5.23	[0.00; 11.56]
α_B	352	195	[37; 332]	8.6e-6	7.9e-6	[6.2e-6; 9.4e-6]	-	-	-
α_C	879	509	[369; 917]	6.8e-6	4.5e-6	[3.2e-6; 6.5e-6]	-	-	-
α_D	327	501	[349; 1050]	2.4e-6	3.5e-6	[2.4e-6; 5.3e-6]	-	-	-
α_E	339	259	[49; 343]	6.6e-7	6.6e-7	[5.2e-7; 7.2e-7]	-	-	-

Note: Exp.: fit on experimental data – M: Median bootstrap – Q1: 1st quartile – Q3: 3rd quartile

Figure captions

Fig. 1. Flowchart for the analyses performed in this work

Fig. 2. Semivariograms for the different correlation models considered in this work (situation without measurement error)

Fig. 3. Boxplots of the estimated scale of fluctuation when the actual correlation model and the analytical model are both Gaussian and the variability of the parameter is equal to 0.15

Fig. 4. Empirical semivariogram for which the correlation matrix is provided in Table 4

Fig. 5. Results of investigations with a measurement error with $\sigma_{par} = 0.05$

Fig. 6. Results of investigations with a measurement error with $\sigma_{par} = 0.15$

Fig. 7. Longitudinal section of the beams (dimensions in mm)

Fig. 8. Cross-section of the beams (dimensions in mm)

Fig. 9. Empirical semivariograms and results of bootstrapping